Journal of the Korean Society for Nondestructive Testing
Vol. 26, No. 6 (2006. 12)

Novel Laser Ultrasonic Receiver for Industrial NDE

B. Pouet†, S. Breugnot and P. Clémenceau

Abstract A new laser-based ultrasonic receiver that is based on multi-channel interferometry is shown to be well suited for robust and sensitive detection of ultrasound in industrial environment. The proposed architecture combines random-quadrature detection with detector arrays and parallel multi-speckle processing. The high sensitivity is reached, thanks to the random phase distribution of laser speckle caused by surface roughness. High-density parallel signal processing is achieved by using a simple demodulation technique based on signal rectification. This simple detection scheme is also demonstrated for rejection of the laser intensity noise, making possible the use of lower cost laser without reduction in performances. Results demonstrating this new principle of operation and its performances are presented.

Keywords: Speckle, Ultrasound, Quadrature, Interferometer, Laser

1. Introduction

In large volume production processes, close attention to manufacturing tolerances can significantly impact manufacturing costs. NDT, previously carried out offline at the end of the production cycle, must now be carried out on-line at early stages in the manufacturing process in order to measure tolerances and to control processes. Real time measurement of product integrity or the early detection of products not meeting specifications provide the manufacturer feedback that they use to control process performance as well as to remove anomalous parts from the process. Ultrasonic technologies have been used for decades for offline measurements. Conventional ultrasonic inspection is based on piezoelectric emitter and receiver coupled to sample by liquid or gel. In order to reach faster inspection rate or to be capable of online measurements, a non-contact technique is preferred. Non-contact ultrasonic techniques that are now becoming broadly used includes: air-coupled transducer, EMAT (electro magnetic acoustic transducer) and LBU (laser-based ultrasonics). EMATs require the inspected material to be metallic and are limited to few millimeters lift-off due to the rapid exponential decay of the electromagnetic force from the surface. Air-coupled transducers are limited to lower frequencies, typically below the MHz due to the high ultrasonic attenuation in the air and the high impedance mismatch. On the other hand, LBU is a remote technique that can operate with stand-off distance up to a meter or more, over a broad frequency bandwidth, from kHz up to GHz. Despites these advantages, LBU have been mostly limited to laboratory application.

LBU is now becoming a more mature technology, making the transition from research laboratory equipment to industrial on-line measurement system. Over the past six years, Lockheed Martin Aeronautics has increased its NDT capacity by nearly ten-fold for the

Received: October 15, 2006, Accepted: Novemver 25, 2006. Bossa Nova Technologies; 606 B Venice Blvd, Venice, CA, 90291 USA. † Corresponding author: bpouet@bossanovatech.com

inspection of CFRP (carbon fiber reinforced plastics) structural parts, by replacing its conventional ultrasonic inspection system with a LBU inspection system, (Voillaume et al, 2006). In the steel manufacturing industry, LBU is used for measuring wall thickness and eccentricity of seamless tubes in production, leading to substantial savings in raw materials and energy, (Jeskey et al, 2004).

Requirements for laboratory measurement are quite different from requirements for online measurement. To be attractive for industrial applications, the LBU system must be very sensitive, but it must also be robust, requires low maintenance and should be able to adapt easily to the industrial environment. Ultimately, the overall cost of the LBU system will be the deciding factor. To date, the high cost is the significant impediment of LBU systems. A LBU system is typically made of a generation unit and a detection unit. The generation unit is essentially a short pulse laser with sufficient power to adequately generate ultrasound in the material. The detection unit typically includes a detection laser and an interferometer. The detection unit is the most critical and its performance and cost will characterize the LBU system. Various optical interferometers have been developed and extensively reviewed, (Dewhurst and Shan, 1999). Adaptive or compensated interferometers based on two-wave mixing in a photorefractive crystal, (Ing and Monchalin, 1991), are becoming a valuable tool for R&D laboratories. To date, adaptive interferometers have not yet been integrated into industrial inspection system, mainly because of their limited response time. LBU industrial inspection systems are still mostly based on the confocal Fabry-Pérot interferometer (Fiedler, 2001). Recent developments also aimed at reducing the cost of the detection laser (Blouin et al, 2005).

Further development on the interferometer is still needed in order to make LBU system more cost effective. Recently, a new type of laser ultrasonic receiver, based on multi-channel quadrature interferometric detection was introduced. This receiver was specifically designed to respond to needs associated with LBU measurement in industrial environments. In this paper the principle of operation of this new laser ultrasonic receiver is described and experimental measurements are carried out to demonstrate its ability to inspect optically rough surfaces and achieve high sensitivity despite of using low cost laser.

2. Quadrature Interferometer

2.1 Principle of Operation

Quadrature interferometers are two-beam interferometer that uses two interference fields 90° out-of-phase. Various optical setups have been proposed to achieve this 90° phase difference (Scruby C.B. and Drain, 1990). Fig. 1 shows an example of an optical setup, where the 90° phase difference is introduced by interfering a circularly polarized reference beam and the linearly polarized beam reflected back from the sample. The signal from the two detectors can be expressed as:

$$i_{D1} \propto I_{obj} + I_{ref} + 2\sqrt{I_{obj} I_{ref}} \cos[\phi_{LF}(t) + \varphi_{UT}(t)] \quad (1.a)$$

and

$$i_{D2} \propto I_{obj} + I_{ref} + 2\sqrt{I_{obj} I_{ref}} \sin[\phi_{LF}(t) + \varphi_{UT}(t)] \quad (1.b)$$

The signal of interest is the small-amplitude and high-frequency phase variation $\varphi_{UT}(t)$ that is induced by ultrasounds reaching the sample surface: $\varphi_{UT}(t) = 4\pi\delta(t)/\lambda$, with $\delta(t)$ the out-of-plane surface displacement and λ the laser wavelength. The phase $\phi_{LF}(t)$ is the low frequency component of the phase and fluctuates between 0 and 2π. I_{obj} and I_{ref} correspond to the intensities of the object beam and reference beam, respectively.

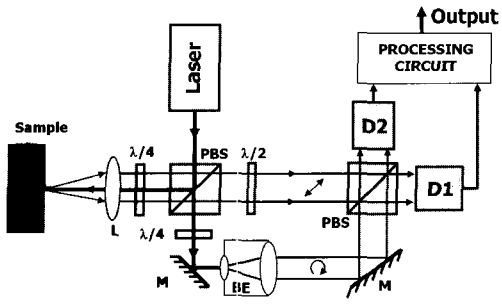

Fig. 1 Schematic of a quadrature detection interferometer: L, focusing lens; PBS, polarization beam splitter; M, mirror; BE, beam expander; D1 and D2, photodetectors.

By properly combining the two quadrature signals i_{D1} and i_{D2}, the ultrasonic surface motion can be extracted. Depending on the signal processing used, the output signal can be proportional to the displacement, the displacement-square or the velocity of the surface motion. Fig. 2 shows the schematics for displacement demodulation and displacement-square demodulation. The architecture for velocity demodulation is not described here, but it is similar to the amplitude demodulation architecture where the low-pass and high-pass filters are replaced by all-pass and derivative filters. After demodulation, the sensitivity to the high-frequency ultrasonic signals is independent of the large amplitude phase variations, $\phi_{LF}(t)$, occurring at lower frequencies.

Quadrature interferometers have been around for more than two decades (Reibold and Molkenstruck, 1981) but they have been of limited use for the detection of small ultrasonic signal, because of the limited performance of high-frequency electronics, mainly the multiplier (mixer) circuits. Multipliers with high-frequency bandwidth, low-noise and extended dynamic range are now available, making quadrature interferometers well suited for high sensitivity ultrasound detection.

2.2 Detection on Rough Surfaces

For industrial application, the inspection must be done on unprepared and generally optically rough surfaces. In this condition, the light collected back by the interferometer is only a small fraction of the incident probe laser and it is highly speckled. The speckle nature of the collected beam limits the interferometer sensitivity. Speckles are characterized by a random distribution of the intensity and the phase (Goodman, 1984). From the speckles statistic we know that the speckle intensity follows a negative exponential function and that the speckle phase is equally distributed between 0 and 2π. Thus in eqn. (1), the phase $\phi_{LF}(t)$ includes both the low-frequency time variation caused by strong disturbance (i.e. air current, vibration, whole body motion or thermal gradient) and the spatial random variation from the speckles. Single

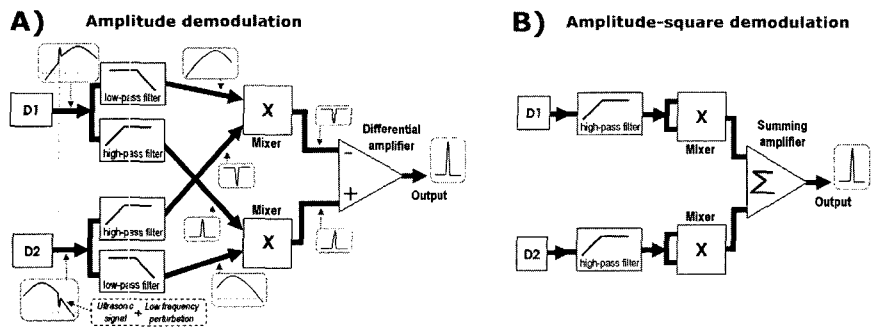

Fig. 2 Demodulation of quadrature signals with the output signal proportional to: A) displacement and B) displacement square.

speckle detection guaranties that $\phi_{LF}(t)$ is spatially uniform, but it limits considerably the amount of light collected. Because of the negative exponential intensity distribution of speckles, the chance to capture a single bright speckle is less than to capture a single dark speckle, resulting in frequent signal dropouts. Fig. 3 shows the results of simulations, assuming a uniformly scattered speckled field and with the reference beam intensity much stronger than the object beam intensity. By increasing the number of collected speckles, the object beam intensity increases proportionally to the number of speckle, but the demodulated signal increases slower because of the speckle random phase distribution. Nevertheless, using a larger aperture for increasing the number of collected speckles still leads to improvement in the signal-to-noise ratio for weak object beam. To increase the number of speckles also reduces the signal intensity fluctuations, leading to less dropouts. The speckle structure of the light also increases the alignment accuracy for the detectors. Indeed, with for accurate quadrature detection, the two detectors must see exactly the same interference field with only a 90° difference. Thus, the two detectors must see exactly the same speckles. This requirement can be challenging if many speckles are collected on the detector.

In order to increase the interferometer sensitivity and to reduce the signal dropouts, the two single-element detectors can be replaced by two detector arrays (Pouet et al, 2006). The optical setup is the same as in Fig. 1. The reference beam expander is adjusted to insure that the whole detector array is illuminated. Parallel processing for demodulation of every channel is now required. The demodulated signals are then summed to generate the final output signal. Amplitude and velocity demodulations are not the best suited for parallel processing because they rely on cross-multiplications between the two quadrature signals. They require seeing exactly the same speckles in order to work properly. On the other side, the amplitude-square demodulation is better suited for high-density parallel processing and not as critical to quadrature alignment.

The integration of detector arrays and their associated parallel demodulation circuitry in the interferometer set-up of Fig. 1 is equivalent to transforming the single interferometer into a multitude of interferometers, looking at the same location and working simultaneously. We showed on Fig. 3 that by collecting more speckle on a detector element, the signal strength increases, but not as quickly as the collected intensity. By increasing the number of detector elements with their associated parallel demodulation circuitry, the signal strength increases proportionally to the number of element (intensity collected). Similarly, the likelihood of signal dropouts decreases very quickly by increasing the number of elements. Using eight detectors was shown to reduce the probability of fading by a factor 100,000 compared to single detector system (Weeks et al, 1998).

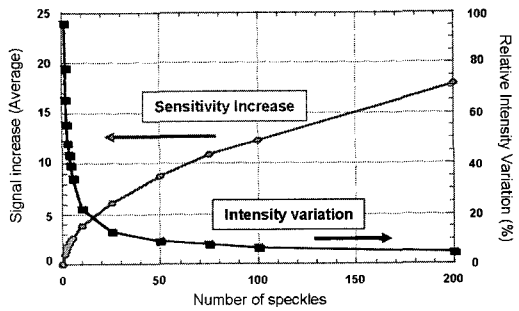

Fig. 3 Averaged value and relative variation of the demodulated signal strength versus the number of collected speckles. Simulation results assuming uniformly distributed speckles.

3. Multi-Detector Random Quadrature Interferometer

As indicated above, detector array with the highest possible number of element is desired for high sensitivity measurement on optically rough surfaces. It is thus important for the signal demodulation to be as simple as possible

and well suited for high-density integration. Furthermore, for use in industrial environment, the optical setup and demodulation scheme should not require too stringent optical alignment and stability conditions. As indicated earlier, the displacement-square demodulation is better suited to high-density integration that the amplitude and velocity demodulations. Nevertheless, the amplitude-square demodulation requires the use of multiplier (mixer) for the squaring process. Multiplier circuits are pricey components and their packaging choice is limited, making very compact design challenging. Furthermore, the squaring process reduces the signal dynamic. To overcome these limitations, we developed a random-quadrature interferometer that uses an approximated demodulation technique based on signal rectification. Rectification is much simpler to implement electronically than squaring and it does not suffer the reduction in signal dynamic. Furthermore, a rectifier can be built with a variety of off-the-shelf low cost electronic components, facilitating the integration into high-density processing circuitry.

The interferometer setup for the random-quadrature interferometer is shown in Fig. 4. Compared to Fig. 1, the interferometric scheme is simplified by removing the quadrature detection requirement. Two detector arrays are used in order to detect all the light available, but it is not required for proper operation of the interferometer. The signal from an element, n, of the photodiode arrays is:

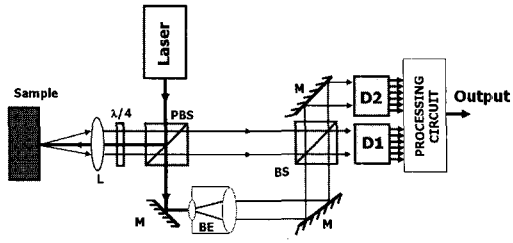

Fig. 4 Schematic of the multi-channel random-quadrature interferometer: L, focusing lens; PBS, polarization beam splitter; BS, beam splitter; M, mirror; BE, beam expander; D1 and D2, photodetector arrays.

$$i_D(n) \propto I_{ref} + 2\sqrt{I_{obj(n)} I_{ref}} \cos[\phi_{LF}(t,n) + \varphi_{UT}(t)] \tag{2}$$

We have assumed that the reference intensity is uniform on the photodiode arrays and much stronger than the object intensity. Every signal is then processed according to the demodulation scheme shown in Fig. 5. The signals are high-pass filtered, amplified and rectified before being summed. For small high-frequency ultrasonic displacement, $\delta(t) << \lambda$, the output signal after processing becomes:

$$V_{Out}(t) \propto 2\sqrt{I_{ref}} \cdot |\varphi_{UT}(t)| \cdot \sum_{N} \sqrt{I_{obj(n)}} |\sin(\phi_{LF}(t,n))| \tag{3}$$

Where N is the number of detector elements. For large number of elements, assuming that the

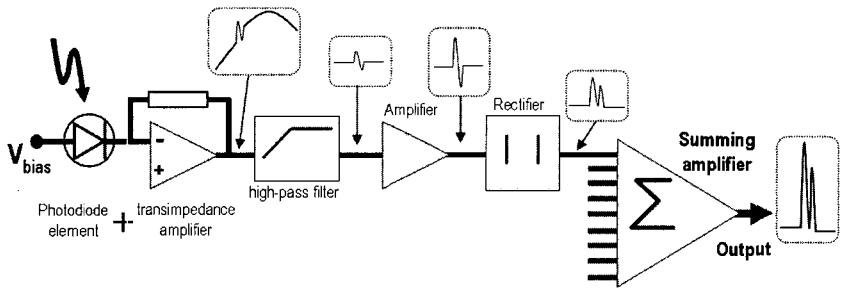

Fig. 5 Schematic of the simplified demodulation used for the multi-channel random-quadrature detection.

speckle phase is uniformly distributed, then the output signal averages out to:

$$V_{Out}(t) \propto 2N \cdot \sqrt{I_{ref} \cdot \langle I_{obj} \rangle} \cdot |\varphi_{UT}(t)| \cdot \frac{2}{\pi} , \qquad (4)$$

$\langle I_{obj} \rangle$ is the speckle average intensity. This multi-channel random-quadrature interferometer exhibits near ideal sensitivity. Compared to the very best sensitivity that could be reached with an "ideal" stabilized Michelson interferometer, that would be capable to stabilize for every speckle, the signal is only reduced by the factor $2/\pi$. We have assumed in eqn. (4) that the speckle is fully resolved by the detector array: one speckle per detector element. If there are more speckles per detector element, the demodulation is still valid but its efficiency is slightly reduced according to the simulation results shown on Fig. 3.

For detector array with small number of elements, the amplitude of the output signal will fluctuate depending on the speckle phases. Fig. 6 shows the fluctuation in time of the output signal for an interferometer with a 25-element detector array, with approximately 10 speckles per element. The speckle phase was made to fluctuate by more than 2π by blowing hot air toward the experiment. Despite the relatively small number of detector elements used for averaging out the random speckle phase distribution, the signal amplitude is fairly stable and fluctuates by no more than 20% from its mean value. An example of ultrasonic signals recorded with a 25-channel random-quadrature interferometer is shown in Fig. 7. A small amplitude ultrasonic pulse is generated with a standard 5 MHz, 0.5 inch diameter, piezoelectric transducer attached to a 0.5 inch thick aluminum plate. The sample surface was sandblasted in order to get a uniform optically rough surface. A 25-channel random-quadrature interferometer with a 70 mW CW laser at λ=532 nm was used for detection. Fig. 7 shows both the single shot signal and the 100-average signal acquired with a detection bandwidth [100 kHz – 10 MHz]. The maximum displacement amplitude of the first echo corresponds to 0.3 nm. Four echoes are clearly visible on the single shot measurement.

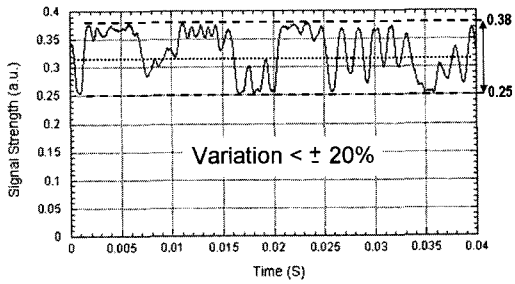

Fig. 6 Fluctuation in the output signal amplitude for the 50-channel interferometer caused by changes in the speckle phases. Phase change was induced by blowing hot air toward the interferometer.

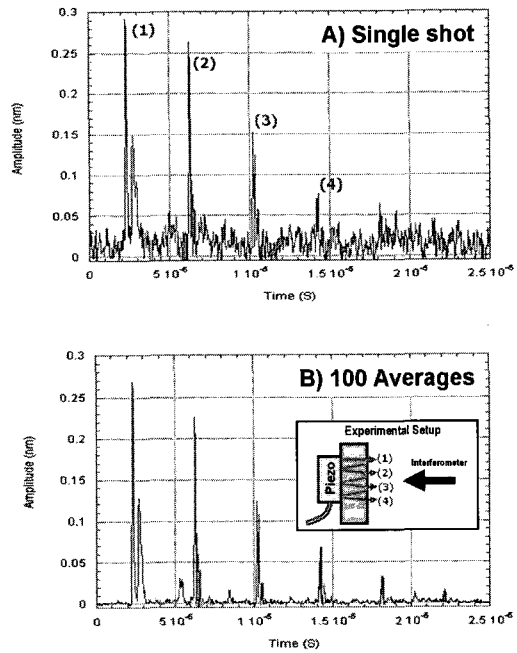

Fig. 7 Ultrasonic surface displacement measured by a 25-channel random-quadrature interferometer: A) Single shot measurement and B) 100-Average measurement. The ultrasonic pulse is generated by a 5 MHz transducer propagating through a 0.5 inch thick aluminium plate. The aluminium surface was sandblasted in order to get a uniformly scattering rough surface.

4. Intensity Noise Rejection

For the interferometer to achieve the theoretical sensitivity limit, we must ensure that the shot noise is the dominant noise source in the system. The shot noise is the quantum noise due the light-to-electrical conversion in the photodiode and it increases with the square root of the intensity on the detector. Other noise sources that may degrade the interferometer sensitivity are: electronic noise, laser phase noise and laser intensity noise.

The electronic noise is independent of the intensity on the detector and in well designed electronics it is set by the first amplifier stage: the transimpedance amplifier as shown in Fig. 5. The noise level of the transimpedance amplifier determines the minimum level of light that can be detected, generally referred as NEP (noise equivalent power). The transimpedance amplifiers we built for the multi-channel detector exhibit a NEP=7.9 $pW/\sqrt{Hz}$, corresponding to 25 μW over the 10 MHz detection bandwidth. By using a reference beam intensity of 100 μW per element, the effect of the electronic noise can be neglected because it will only add 3% of noise to the shot noise limit.

The phase noise is related to the coherence of the laser and needs to be considered when the path difference between the interfering beams is no longer small compared to the coherence length of the laser. Here, the coherence length requirement is not critical since the signal and reference paths could be made nearly equal. With current laser technology, laser coherence length of few meters and more are commonly available. Using a 200 mW single longitudinal mode DPSS laser (G4plus200, manufactured by Elforlight Ltd.) and a path difference of 1meter, we saw no evidence of phase noise. The laser phase noise will thus be considered negligible.

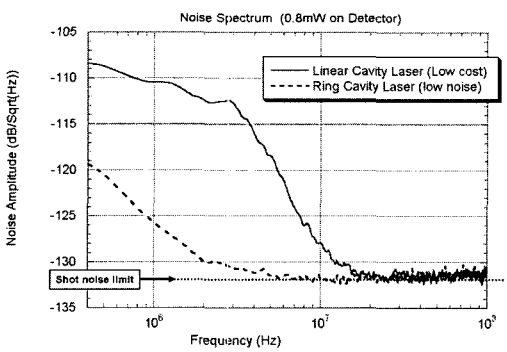

Fig. 8 Frequency spectrum of noise for 800 μW laser power on detector. Comparison between linear cavity laser and ring cavity laser.

The laser intensity noise is more critical. At frequency below few MHz, the intensity noise can quickly become the limiting factor for the interferometer sensitivity. Fig. 8 compares the noise spectrum of two single longitudinal mode DPSS lasers: a linear cavity and a ring cavity. The noise spectrum was recorded with 800 μW on a photodiode. The detector electronic noise was well below the shot-noise limit corresponding to 800 μW. As expected, the lower cost linear cavity laser exhibits more intensity noise than the ring cavity laser. At 1 MHz the linear cavity laser exhibits an intensity noise 20 dB above the shot noise limit. Nevertheless, both lasers exhibit increasing intensity noise at lower frequencies. For interferometer optimization, the reference beam intensity is adjusted such that the shot noise is superior to the electronic noise, typically 100 μ W/element for our application. We see from eqn. (2) that with the condition $I_{ref} >> I_{obj}$, both the modulation amplitude and the shot noise increase with the square-root of the reference intensity. Unfortunately, the laser intensity noise, increasing linearly with the intensity, can quickly limit the interferometer sensitivity. Rejection of intensity noise is needed in order to reach the expected interferometer sensitivity in the frequency range [100 kHz – 10 MHz]. Laser intensity noise rejection is generally achieved by using a balanced detection scheme (Scruby C.B. and Drain, 1990). With balanced detection, two interference signals of same amplitude, but

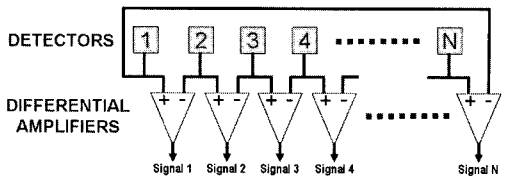

Fig. 9 Differential detection scheme for laser intensity noise rejection.

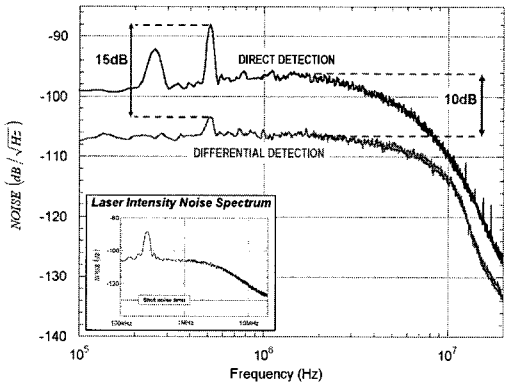

Fig. 10 Frequency spectrum of noise for 250μW/per detector element. Comparison between direct amplification and differential amplification. The intensity noise spectrum of the laser used for this demonstration is also shown.

180° out of phase, are recorded by two photodetectors. The differenced between the two detector outputs gives a "balanced" output, where the common noise has been rejected.

With our multi-detector random-quadrature interferometric scheme the implementation of a classic balanced detection scheme is not very practical. Instead, we can once again take advantage of the speckle random distribution to reject the laser intensity noise and to reach shot noise detection limit. We developed a differential detection scheme that can be simply implemented electronically without any changes of the optical setup shown Fig. 4. This intensity noise rejection scheme is based on the following assumptions: 1) light scattered back from the object is weak compared to the intensity of the reference beam, 2) the intensity of the reference beam is uniform over the detector array and most importantly 3) light scattered back by the object is composed of speckles which have random phase distribution and are not correlated. Fig. 9 shows the principle of operation of the proposed intensity noise rejection scheme. By carrying out this differential detection, the intensity noise that is due mainly from the stronger reference beam intensity is subtracted out. On the other hand, the signal amplitude is increased in average by $\sqrt{2}$, because the two detectors see uncorrelated speckle phases. It must be pointed out that the shot noise also increases by $\sqrt{2}$. This differential detection scheme is easily integrated in our demodulation circuitry by replacing the amplifiers in Fig. 5 with differential amplifiers.

An example of laser intensity noise rejection is shown on Fig. 10 where we compare the noise spectrum at the output of a 50-channel random-quadrature interferometer with standard amplification and with differential amplification, for 250 μW of the reference beam intensity per elements. The laser used for this experiment exhibited strong intensity noise below 10 MHz, with a noise peak at 260 kHz, as shown on Fig. 10. After demodulation, the noise peak appears at 520 kHz because of the rectification process, which doubles the frequency. A 15 dB reduction of this noise peak is achieved with the differential detection scheme. A small noise peak is still visible at 520 kHz, mostly due to the spatial variation in the reference beam intensity.

An example of LBU measurement on a 20 mm thick steel sample with unprepared surfaces is shown in Fig, 11. The ultrasounds were generated on one side by laser ablation resulting from the absorption of a 200 mJ, 10 nS pulse duration Nd:YAG laser @1.06 μm and focused to a 1 mm spot diameter. The 50-channel random-quadrature interferometer used a 70 mW CW laser @ 532 nm and was looking at the opposite surface, at the epicenter. The stand-off distance between sample and interferometer was 10 cm

and the effective collecting aperture was 65 mm^2. Fig. 11 shows a single shot signal and the signal after 4 averages. The detection bandwidth was [100 kHz - 10 MHz] and the 1st echo amplitude corresponds to a 1.8 nm displacement.

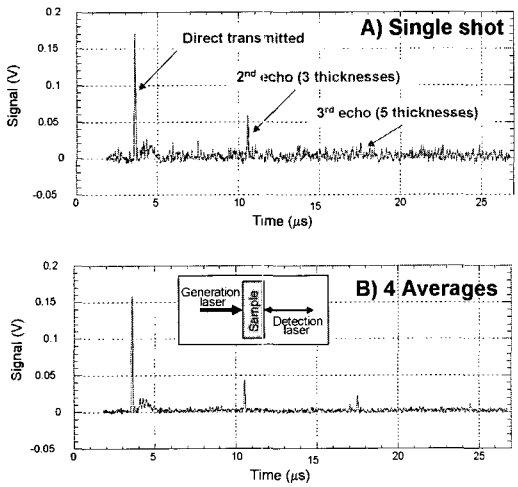

Fig. 11 Through-transmission LBU measurement with a 50-channel random-quadrature interferometer on a 20 mm thick steel plate: A) Single shot measurement and B) 4-average measurement. The amplitude of the 1st echo corresponds to a 1.8 nm displacement.

5. Conclusion

Multi-channel random-quadrature interferometer is a very attractive receiver for industrial LBU applications. Laser speckle caused by surface roughness generally limits the performance of "classic" interferometers but we showed that with the random-quadrature interferometer laser speckle is taken advantage of in order to build a compact, robust and sensitive interferometer. By increasing the number of channels, the sensitivity and signal stability increase. We demonstrated that high density parallel processing of channel is made possible by the use of a simple demodulation scheme based on signal rectification and that laser intensity noise can also be easily rejected, making this interferometer well suited for cost sensitive applications.

Acknowledgements

This work was supported by the National Science Foundation, DMI-0319425.

References

Blouin A., Carrion L., Padioleau C., Bouchard P., and Monchalin J.-P. (2005) Simple Laser-Ultrasonic System Using a Single Frequency Pulsed Laser Oscillator, *Review of Progress in Quantitative NDE*, Vol. 24, eds D. O. Thompson and D. E. Chimenti, AIP, New York, pp. 265-272.

Dewhurst, R. J. and Shan, Q. (1999) Optical Remote Measurement of Ultrasound, *Meas. Sci. Technol.* Vol. 10, pp R139-R168.

Fiedler, C. J. (2001) Laser Based Ultrasound Technology Assessment, *Review of Progress in Quantitative NDE*, Vol. 20, eds. D. O. Thompson and D. E. Chimenti, AIP, New York, 2001, pp. 308-315.

Goodman, J.W. (1984) *Laser speckle and related Phenomena,* 2nd ed., J.C. Dainty, ed., Vol. 9 of Springer Series in Topics in Applied Physics, Springer-Verlag, Berlin,

Ing, R.K. and Monchalin, J.-P. (1991) Broadband Optical Detection of Ultrasound by Two-Wave Mixing in a Photorefractive Crystal, *Appl. Phys. Lett.* Vol. 59, No. 25, pp. 3233-3235.

Jeskey G., Kolarik R., Damm E., Monchalin J.-P., Lamouche G., Kruger S. E., and Choquet M., (2004) Laser Ultrasonic Sensor for On-Line Seamless Steel Tubing *Process Control, Proceeding of the 16th World Conference on Nondestructive testing*, Montreal.

Pouet B., Breugnot S., and Clemenceau P. (2006) Robust Laser-Ultrasonic Interferometer Based on Random Quadrature Demodulation, *Review of Progress in Quantitative NDE*, Vol. 25, eds D.

O. Thompson and D. E. Chimenti, AIP, New York, pp. 233-239.

Reibold, R. and Molkenstruck, W. (1981) Laser Interferometric Measurement and Computerized Evaluation of Ultrasonic Displacements, *Acustica* Vol. 49, pp. 205-211.

Scruby, C.B. and Drain, L.E. (1990) Laser Ultrasonics: *Techniques and applications*, ed. Adam Hilger, Bristol, UK.

Voillaume H., Simonet D., Brousset C., Barbeau P., Arnaud J.-L., Dubois M., Drake T., and Osterkamp M. (2006) Analysis of Commercial Aeronautics Applications of Laser Ultrasonics for Composite Manufacturing, *Proceeding of the 9th European NDT Conference*, Berlin.

Weeks A. R., Xu J., Phillips R. R., Andrews L. C., Stickley C. M., Sellar G., Stryjewski J. S., and Harvey J. E. (1998) Experimental Verification and Theory for an Eight-Element Multiple-Aperture Equal-Gain Coherent Laser Receiver for Laser Communications, *Applied Optics*, Vol. 37, No. 21, pp. 4782-4788